JMB

REVIEW

Chromatin Fibers, One-at-a-time

Jordanka Zlatanova[1]* and Sanford H. Leuba[2]

[1]*Department of Chemistry and Chemical Engineering Polytechnic University, 6 Metro Tech Center, Brooklyn NY 11201, USA*

[2]*Department of Cell Biology and Physiology, School of Medicine, University of Pittsburgh, Hillman Cancer Center, University of Pittsburgh Cancer Institute Research Pavilion, Pittsburgh PA 15213, USA*

Eukaryotic DNA is presented to the enzymatic machineries that use DNA as a template in the form of chromatin fibers. At the first level of organization, DNA is wrapped around histone octamers to form nucleosomal particles that are connected with stretches of linker DNA; this beads-on-a-string structure folds further to reach a very compact state in the nucleus. Chromatin structure is in constant flux, changing dynamically to accommodate the needs of the cell to replicate, transcribe, and repair the DNA, and to regulate all these processes in time and space. The more conventional biochemical and biophysical techniques used to study chromatin structure and dynamics have been recently complemented by an array of single-molecule approaches, in which chromatin fibers are investigated one-at-a-time. Here we describe single-molecule efforts to see nucleosomes, touch them, put them together, and then take them apart, one-at-a-time. The beginning is exciting and promising, but much more effort will be needed to take advantage of the huge potential that the new physics-based techniques offer.

Corresponding author

Introduction

It has been known for decades that the genomes of eukaryotic cells are organized in interphase as chromatin, a complex between DNA and small, highly basic proteins, histones.[1–4] The basic repeating unit of chromatin structure, the nucleosome, is now well characterized.[5–8] We have also acquired significant knowledge of how nucleosomes form linear arrays, with individual particles connected with stretches of linker DNA. *In vivo*, these nucleosomal arrays bind other proteins, such as linker histones or high mobility group (HMG) proteins, which contribute to the further levels of folding of the chromatin fiber. These levels of folding remain largely unknown.

The recent resurrection of interest in chromatin structure and its dynamics came with the realization that chromatin is much more than just a venue of highly packaged genetic material in the confines of the cell nucleus. Chromatin turned out to be intimately involved in the regulation of the numerous activities of DNA: replication, transcrip-

tion, repair, and recombination. It came as no surprise that chromatin needs to undergo significant structural changes when the cellular machineries that perform all these functions are to access their template, the double-helical DNA. What was not so obvious was that these structural transformations are highly regulated in time and space, and, in turn, regulate DNA functioning. How is chromatin structure regulated, to regulate gene activity? Or are some of the changes in chromatin structure observed upon DNA functioning a mere consequence of gene activity? Actually, there is no *a priori* reason to think that these two scenarios are mutually exclusive; most probably they could each occur in different situations.

The challenge to understand chromatin structure and dynamics and to link chromatin structure to function is enormous. Numerous laboratories worldwide are applying a huge range of biochemical and biophysical approaches in an attempt to unravel chromatin secrets. The research effort nowadays seems to focus on the post-synthetic modifications of both the histones and the DNA. Numerous modifications of individual amino acid residues at specific sites along the histone polypeptide chains are being described, and the enzymatic machineries carrying these reactions are being identified. Attempts are being made to

Abbreviations used: AFM, atomic force microscopy; EM, electron microscopy.

E-mail address of the corresponding author: jzlatano@duke.poly.edu

understand the functional consequences of these modifications and the molecular mechanisms through which they act. Equally intriguing are the mechanisms *via* which methylation of specific CpG dinucleotides in different gene regions is achieved, maintained, and inherited, to affect gene transcription.

The complexities of chromatin structure and its dynamic alterations in response to external and internal stimuli will remain one of the main foci of molecular biology in the years to come. New approaches are being sought and added to the arsenal of existing, more conventional methods used in chromatin research. A whole new battery of single-molecule methods is now emerging in which molecular populations are studied molecule-by-molecule, one-at-a-time.[9,10] These techniques overcome the drawbacks of the population-averaged measurements, in which the differences between individual molecules are masked in the ensemble average; moreover, since the stochastic nature of most biochemical reactions leads to extremely fast loss of synchrony, even when the starting population is synchronized at a certain step of the biochemical pathway, real-time observations of the reaction kinetics are not possible. The new physics-based methods allow unprecedented insights into a host of biochemical reactions involving DNA, RNA and proteins. The aim of this review will be to describe the kinds of single-molecule methods that have been used so far in chromatin research, the questions asked, and the first answers. A glimpse at this emerging field of chromatin research will, we hope, reveal the power of the new methodology in understanding chromatin structure and dynamics.

High-resolution imaging techniques

The first attempts at applying single-molecule approaches to chromatin research involved high-resolution imaging techniques. In these techniques, native, biochemically manipulated, or reconstituted chromatin fibers are imaged and measured, one by one, to give statistically valid data through the observation of huge numbers of individual fibers. Although, strictly speaking, high-resolution electron microscopy (EM) belongs to this class of techniques, we focus here on the more recent atomic force microscopy (AFM) and cryo-EM studies.

Atomic force microscopy

AFM is one of several recent instruments that use sharp probes to obtain images of individual molecules.[11] The AFM uses a sharp tip mounted at the end of a flexible cantilever to raster-scan samples immobilized on an atomically flat imaging surface, like mica, glass, or gold (Figure 1a). Atoms on the apex of the AFM tip interact with atoms on the sample causing deflections of the flexible cantilever; the direction and extent of cantilever deflection at each point of the sample depends on whether the interaction at this specific point is attractive or repulsive, and on its strength.[12–14] These deflections are registered by a laser beam reflected off the back of the cantilever into a photodiode position detector, and the signal is used to produce digital topographic images. The AFM generally has a nanometer lateral resolution when imaging soft biological samples (the resolution is truly atomic with hard materials). In addition, imaging is performed under conditions likely to preserve the structures under investigation: both ambient air and liquid imaging are possible. Even when imaging is done in air, there is a thin layer of liquid water above the sample, thus allowing the imaged molecules to preserve the structurally important water molecules, and thus, their native
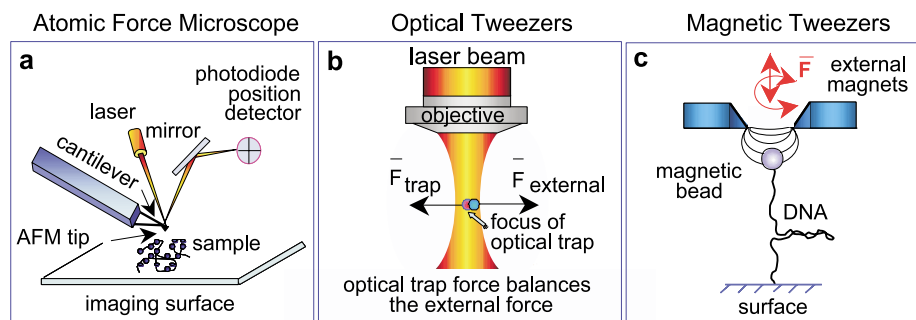
Figure 1. Principle of operation of the AFM, optical tweezers, and magnetic tweezers. (a) AFM. The tip/cantilever raster-scans the biological sample on an atomically flat surface, and a topographic image is created from the changes in the laser signal caused by the deflections of the cantilever; these, in turn, are caused by atomic-level tip/sample interactions. For force spectroscopy, the cantilever is moved in the *z*-direction only, and the deflection of the cantilever is followed as a function of the distance between the tip and the sample. Force is the product of the cantilever deflection and its spring constant (see Figure 6 and its legend). (b) Optical trap. Force is determined by $F = k\Delta x$, where k is the spring constant of the trap, and Δx is the displacement of the bead from the focus of the trap. (c) Magnetic tweezers. A single DNA molecule is tethered between a superparamagnetic bead and a surface. Based on the equipartition theorem, force is determined by $F = lk_{B}T/\langle\Delta x^{2}\rangle$, where l is the distance between the DNA-tethered bead and the surface, k_{B} is Boltzmann's constant, T is the temperature, and $\langle\Delta x^{2}\rangle$ is the Brownian fluctuations of the bead.

structure. The AFM can be used to also mechanically manipulate macromolecules, an application which will be discussed below.

We have recently reviewed in detail the literature on AFM imaging of chromatin.[15,16] Here we will limit ourselves to tabulating some of the more important studies (Table 1) and listing some of the new findings and insights.

AFM imaging of native chromatin fibers solubilized from chicken erythrocyte nuclei by brief micrococcal nuclease treatment and deposited on glass or mica from low-ionic strength buffers revealed fibers with a loose, quite irregular, three-dimensional organization of individual, well-resolved nucleosomes (Figures 2 and 3). Although the path of the linker DNA was only rarely visualized in these images (due to the well-known broadening effect of the AFM tip, which artificially enlarges the nucleosomes), it was clear that the structures were truly three-dimensional, with individual nucleosomes at different heights above the imaging surface. Thus, even at low ionic strength, at their most extended state, chromatin fibers fold in a certain, albeit rather irregular, way. This three-dimensional morphology is quite different from the morphology seen under similar ionic conditions under the EM (Figure 3), presumably due to the better preservation of the native structure in AFM imaging. Chromatin fiber images similar to those obtained by AFM were also recorded by cryo-EM[17,18] (see below); this similarity is of particular importance, since it negates the possibility that the irregular fiber morphology in AFM images may be an artifact of sample/surface interactions.

In an interesting, and, we believe, important twist, chromatin fibers were mathematically modeled based on known structural parameters and assuming straight linkers (similar modeling with similar outcome was first reported by Woodcock *et al.*[19]). The mathematical models were then turned into "fake" AFM images by first simulating the surface deposition process, and then introducing the broadening effect of the AFM tip. Gratifyingly, the simulated AFM images of the mathematical models turned out very similar to (almost indistinguishable from) the actual AFM images of real chromatin fibers.[20–22] Thus, the views that chromatin fibers are organized in a much more irregular way than envisaged by the canonical solenoidal model[23,24] of the "30-nm" fiber gained additional strength. (The term "30-nm fiber" has been widely used to denote the structure of the chromatin fiber at its first level of compaction, beyond the beads-on-a-string morphology observed by EM for fibers deposited from low ionic strength buffers. This term is, however, misleading, since the diameter of the fiber at its most extended state also measures ~30 nm; the actual parameter that distinguishes the extended fiber from the compacted one is the linear nucleosomal density, i.e. the number of nucleosomes per unit fiber length (see below).[22,25–28]

Combining biochemical manipulations of chromatin fibers with AFM imaging of the resulting structures has made some important contributions to our knowledge of the role of individual histone molecules or portions thereof in chromatin structuring. Thus, stripping of linker histones from native fibers results in transforming fiber morphology, from the irregular, three-dimensional arrangement of nucleosomes to a beads-on-a-string appearance[20,21,29] (Figures 2 and 3). Conversely, reconstitution of linker histones onto linker-histone depleted fibers leads to recovery of the native structure.[29] Another series of reconstitution experiments aimed at defining some other molecular determinants of native fiber structure. To that end, fibers mildly digested with membrane-immobilized trypsin were stripped of linker histones to produce substrates that lacked both linker histones and the 26 amino acid residues from the N-tails of histone H3. When isolated linker histones or their globular domains were reconstituted onto such fibers and the reconstitution products were analyzed by AFM imaging, it became clear that the linker histone tails and the N-terminal tails of histone H3 could substitute for each other in recovering the native fiber structure. Either of these tails, in conjunction with the globular domain of linker histones, was necessary and sufficient to reconstruct the original structure.[29] The reconstitution data confirmed and extended the conclusions obtained upon imaging of partially trypsinized chromatin fibers.[30]

Several recent reports used AFM imaging to reveal structure–function connections in chromatin. One report studied the structural consequences of treating reconstituted nucleosomal arrays with the chromatin remodeling complex SWI/SNF, directly demonstrating a change from evenly spaced nucleosomes into disorganized structures.[31] Another important study revealed cooperation between DNA methylation and linker histone binding in compacting methylated fibers.[32] Still another study compared nucleosomal arrays reconstituted on circular templates with either intact or tailless histones, with no apparent difference in overall appearance or in center-to-center internucleosomal distances (Figure 2).[33] The contribution of such studies to our overall knowledge of chromatin structure and function will obviously grow in the future.

The successful future application of AFM to chromatin studies will require further improvement of the spatial resolution in AFM images. So far, the highest resolution reported allowed visualization of individual histone molecules within disrupted nucleosomes,[34] and occasional visualization of the DNA wrapped around the histone octamer.[35] Linker histone binding was observed by cryo-AFM as increased mass at the DNA entry/exit point[36] (see Figure 2), and linker histone addition to stripped mono-, di- and oligonucleosomes from chicken erythrocytes caused the formation of recognizable stem

Table 1. Major results and conclusions from AFM and cryo-EM imaging of chromatin

	Major results	References
A. *AFM imaged substrate*		
Chicken erythrocyte (CE)[a] chromatin fibers	First beads-on-a-string AFM images	115
Nucleosomal arrays reconstituted from histone octamers and 208-18[b] DNA	Beads-on-a-string morphology; center-to-center distances of ~37 nm	112
Hypotonically spread CE nuclei; detergent-treated nuclei from human B lymphocytes; native, dry, or rehydrated samples	Beads-on-a-string morphology in hypotonic spreads; the detergent spreads are supranucleosomal chains; image processing (extraction of cross-sections of nucleosomes at half-maximum height) reveals ellipsoid shape of nucleosomes with an aspect ratio of 1.2–1.4 and a relatively smooth perimeter; the orientation of the virtual ellipsoids is correlated with the direction of the fiber axis, with >50% of nucleosomes aligned with the axis (could be partly due to interaction with glass and/or drying)	116–119
CE chromatin fibers at different salt concentrations; unfixed or glutaraldehyde-fixed chromatin fibers; native or LH-depleted fibers	Loose, three-dimensional, 30 nm irregular structures even in the absence of salt; beads-on-a-string fibers seen only in H1/H5-depleted fibers. At 10 mM NaCl the fiber condenses slightly; at 80 mM NaCl highly compacted, irregularly segmented fibers	20,21,120
rDNA minichromosomes from *Tetrahymena thermophila*	Condensed 30 nm fibers near center of mica; extended fibers at mica periphery with partially dissociated nucleosomes; clusters of smaller particles within these nucleosomes suggested to be individual histone molecules	34
Progressively trypsinized CE chromatin fibers; reconstitution of CE chromatin fibers depleted of LH or of LH and the N-tails of H3 with either intact H5 or GH5	Cleavage of LH tails results in fiber lengthening whereas cleavage of H3 N-tails flattens the fiber; zigzag morphology persists at later stages of digestion and is attributed to retention of the globular domain of LH in fiber; the three-dimensional organization of nucleosomes in extended (low ionic strength) chromatin fibers requires the globular domain of LHs and either the tails of LH or the N-terminal tails of H3	29,30
LH-stripped mono-, di-, and oligonucleosomes from CE	Occasional visualization of the DNA wrapped around the histone octamer and of linker DNA; occasional superbeads observed	35
Nucleosomes reconstituted on linearized plasmids and HeLa core histones	Nucleosome positioning recognized; H1 addition reportedly compacts the dinucleosome and forms stem structures	37
Chicken erythrocyte chromatin	Cryo-AFM gives higher resolution of chromatin fibers; at DNA entry/exit point, added mass suggests visualization of linker histone	36
Chromatin fibers from control or poly(ADP-ribosyl)ated CE nuclei; *in vitro* poly(ADP-ribosyl)ated fibers	Poly(ADP-ribosyl)ation induces decondensation of chromatin structure which remains significantly decondensed even in the presence of Mg^{2+}: Mg^{2+} cannot substitute for linker histones to induce compaction	121
HeLa mononucleosomes; nucleosome arrays reconstituted from modified 208-12 and core histones; the arrays remodeled with hSWI/SNF	Dimers from SWI/SNF-treated mononucleosomes have ~60 bp more weakly bound by histones than those from control mononucleosomes; control arrays with evenly spaced nucleosomes are disorganized by SWI/SNF; compact dimers could not be positively identified within these arrays	31
Chromatin fibers isolated from cells with normal or elevated levels of m^5C; nucleosome arrays reconstituted from either unmethylated or *in vitro* methylated 208-12 and core histones; additional reconstitution of LH	DNA methylation induces chromatin compaction only in the presence of bound LH; AFM results substantiated by MNase digestion patterns and sucrose gradient centrifugation. AFM imaging can visualize alternative nucleosome positioning on adjacent 208-bp repeats (the distribution of center-to-center distances on 208-12 is bimodal)	32
Nucleosome arrays reconstituted from 208-18 and either histone octamers, H3/H4 tetramers or the histone-fold protein HMf from *Archaea*	The HMf-nucleoprotein complexes are *bona fide* chromatin structures. The HMf-containing mononucleosomes are less stable than the canonical octasomes	113
Nucleosomal arrays reconstituted from a 5.4 kbp circular template and control or totally tailless recombinant histones	Beads-on-a-string; center-to-center distance frequency distributions indistinguishable for control and tailless reconstitutes	33
Control and hyperacetylated mononucleosomes isolated from HeLa cells	Low force images of control and hyperacetylated mononucleosomes appear to be the same; large imaging force causes flattening of mononucleosomes; reduction to normal force allows control mononucleosomes to regain original heights, whereas hyperacetylated mononucleosomes fail to do so	122

(continued)

Table 1 Continued

	Major results	References
B. *Cryo-EM imaged substrate*		
SV40 minichromosomes	In high-salt buffer (130 mM NaCl), condensed globules of ~30 nm in diameter, composed of closed packed nucleosomes. At low salt, the globules open, first into 10 nm filaments, then into nucleosome strings; a liquid drop model for the condensed minichromosomes is suggested	41
Mononucleosomes reconstituted on a 256 bp fragment with duck erythrocyte histone octamers; no linker histone	Particle with 1.61($\pm$0.15) left-handed superhelical turns; DNA arms bend away from the core particle; entry/exit angle ~33°	123
Small oligonucleotides from CE at different ionic strength	Salt-induced compaction of trinucleosomes occurs by a reduction in the entry/exit angle; the distance between consecutive nucleosomes is not reduced. The three-dimensional zigzag appearance of polysomes is preserved even at 40 mM; no evidence of solenoidal arrangements is found	17
CE and COS-7 cell chromatin fibers; nucleosome arrays reconstituted on 208-6 by salt dialysis	The stem-like organization of the entering and exiting linker DNA segments clearly visualized in the presence of linker histones; the stem motif is proposed to direct the arrangement of nucleosomes and linker DNA within the fibers, establishing the basic three-dimensional zigzag folding pattern at all levels of compaction	18
Transcribing SP6 RNA polymerase arrested at unique positions in a nucleosome core reconstituted on 227 bp fragments	DNA remains wrapped on the histone octamer during passage of polymerases. Two intermediates identified: "open transcriptional intermediate", in which RNA polymerase is located on DNA partially displaced form histones; and "closed transcriptional intermediate", in which the same DNA segment harbors both the polymerase and the octamer	124
Polynucleosomes isolated from chicken granulocytes and from COS-7 cells imaged in 20 mM NaCl	Differentiated granulocytes: very compact fibers, with nucleosome disks predominantly at the periphery; entry/exit sites oriented towards fiber interior; thicker fibers originating from folding of a fiber back on itself (see Figure 4). Actively proliferating COS-7 cells: open zigzag organization, no thick fibers (see Figure 4)	49
Isolated core particles from calf thymus (146 bp of DNA)	Spermidine and salt led to formation of dense aggregates of variable supramolecular organization: amorphous, stacked core particle columns, or liquid crystalline phases, in which the columns are either aligned in parallel or form hexagons	125
167 bp or 146 bp linker histone depleted-mononucleosomes from CE or calf thymus	A new lamellar mesophase of particles is described, in which columns of core particles align in bilayers separated from each other by a solvent layer; an attempt is made to link the formation of these bilayers to the tails of H2B and H2A protruding from the crystal structure of the core particle	126

[a] CE, chicken erythrocyte.
[b] 208-18, a tandemly repeated DNA sequence that has a nucleosome-positioning 208 bp sequence repeated 18 times.[127]

structures[37] (for more on the stem structure, see below).

Cryo-electron microscopy

In cryo-EM, samples are observed in their fully hydrated, unperturbed three-dimensional structure, freely suspended in a layer of vitrified water; vitrification (solidification without ice crystal formation) is achieved by an extremely rapid plunging of the sample holder into liquid nitrogen.[38,39] The biological samples are neither stained nor fixed; possible artifacts due to interactions of the sample with the imaging surface (as in conventional EM, or the AFM) are totally avoided. The main drawback of the technique is that the image contrast cannot be boosted by staining or shadowing, and sophisticated image analysis and reconstruction is often required for obtaining detailed high-resolution images. The technique and its application to chromatin research have been recently reviewed.[40]

Cryo-EM was used as early as 1986 for imaging of chromatin fibers.[41] Although the number of laboratories in the chromatin field that are using this technique is very small, its contribution is significant (for a list of published work, see Table 1, and for some representative images, see Figure 4).

Cryo-EM images of mono-, di-, and higher oligonucleosomes, isolated from cells or reconstituted *in vitro*, have provided, together with AFM-acquired images, a major incentive to rethink our ideas of

Native fibers   Reconstituted fibers
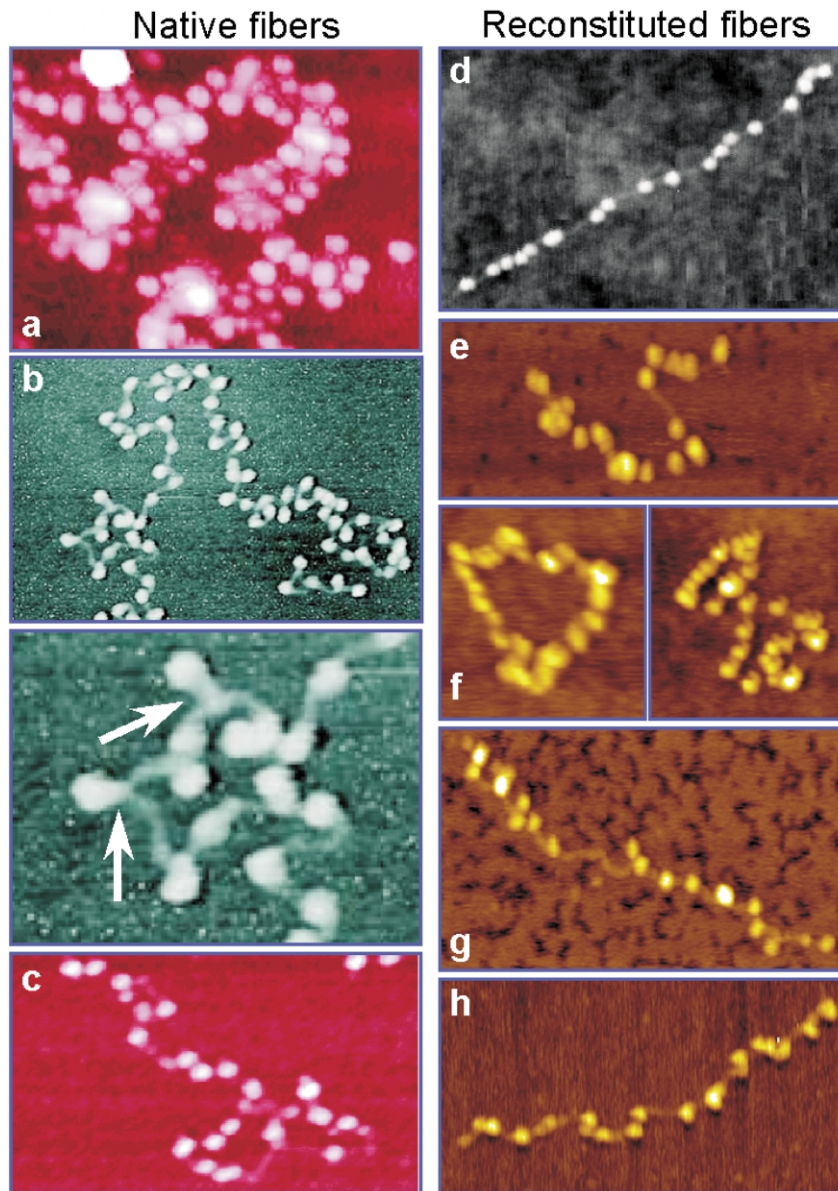
Figure 2. Some example AFM images of chromatin fibers. Left-hand column (a–c), fibers isolated from nuclei; right-hand column (d–g) reconstituted nucleosomal arrays. a, Unfixed chicken erythrocyte chromatin fiber imaged on glass in air (S. Leuba & G. Yang, unpublished). b, Upper panel, cryo-AFM image of a chicken erythrocyte chromatin fiber on mica.[36] Nucleosomes are well resolved along with linker DNA. Lower panel, zoom of a portion of the fiber in the upper panel, suggesting visualization of linker histone. Arrows point to increased mass at DNA entry/exit sites. (Courtesy of Z. Shao). c, Linker histone-depleted chicken erythrocyte chromatin fiber on mica in air (S. Leuba, unpublished). d, Nucleosomal array, reconstituted from 208-18 DNA and core histones by salt dialysis, and imaged on mica in air. Reprinted with permission from Allen *et al*.[112] Copyright 1993 American Chemical Society (courtesy of M. Allen). e, A similar sample imaged under similar conditions in another laboratory.[113] f, Circular plasmids reconstituted with recombinant assembly factors and intact recombinant core histones (left-hand panel), or core histones missing their N-terminal extensions (right-hand panel). Reprinted from An *et al*.,[33] with permission from Elsevier Science. g, H3/H4 tetrasome array, reconstituted from 208-18 DNA and H3/H4 tetramers by salt dialysis, imaged on mica in air. h, Nucleosomal array, reconstituted from 208-18 DNA and archaeal-histone HMf (histone from *Methanothermus fervidus*) by salt dialysis, imaged on mica in air. e, g, h, Reprinted from Tomschik *et al*.,[113] with permission from Elsevier Science.

how the chromatin fiber is organized at levels higher than the level of linear arrangements of nucleosomes (see also above).[22,25–28] Although a detailed discussion of this issue falls outside the scope of this review, we will briefly mention it because of its overall importance to the entire chromatin structure field.

Both AFM and cryo-EM images showed that the chromatin fiber appears, at low ionic strength, as a loose three-dimensionally organized, irregular, zigzag arrangement of nucleosomes, with no substantial evidence for the formation of regular solenoids. The fiber can be successfully modeled on the basis of a few known structural parameters of the core
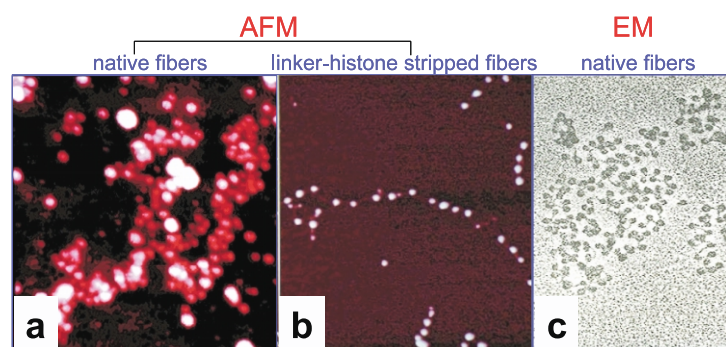
Figure 3. Comparison between AFM (a and b) and EM (c) images. a, Unfixed chicken erythrocyte chromatin fiber imaged on glass in air.[20] b, Linker-histone stripped chicken erythrocyte chromatin fiber on mica in air.[20] Images (a) and (b) copyright (1994) National Academy of Sciences, USA (c) EM micrograph of rat liver chromatin fibers. Reprinted from De Murcia & Koller,[114] with permission from Elsevier Science. In all three cases, the fibers were deposited onto the imaging surfaces from low-ionic strength buffers, with no added salt.

particle, variable linker lengths, and a variable angle between entering and exiting linker segments.[17,19–21,42–46] The trajectory of the linker DNA in the model is straight, as directly visualized in cryo-EM images. The first level of salt-induced compaction of such fibers occurs by decreasing the entry/exit angle.[17,18,25] The importance of linker histones in chromatin structure has also been directly demonstrated in both AFM and cryo-EM images.[18,20,21] Using cryo-EM, Woodcock and co-workers[17,18] (reviewed by Grigoryev[47]), were able to convincingly visualize the stem structure formed by the nucleosome linkers at the entry/ exit DNA site in a nucleosome array. The linker stem formation is due to linker histone binding at the entry/exit DNA site.[48] This structure gives nucleosomes in a fiber a "tennis-racket" type of appearance: the DNA segments form an inter-section zone about 8 nm from the center of the nucleosomes, and this zone (stem) extends for 3–5 nm before the linker DNA segments diverge from each other. The linker DNA stem together with the linker histone are suggested to form a unique motif that directs the higher-order folding and compaction of chromatin along the 30 nm fiber axis in an accordion-like manner.[18]

Another highly significant insight that came from cryo-EM imaging concerns the clear-cut differences seen in stem formation and compaction above the "30-nm" level in proliferating *versus* differentiated cells. As Grigoryev *et al.*[49] demon-strated, chromatin from proliferating cells that contains a normal amount of linker histones seems to form shorter stems and more open linkers resulting in a more extended chromatin fiber. In addition, this chromatin does not self-associate but remains in an open three-dimensional zigzag conformation. On the other hand, fibers from highly differentiated cells, like chicken granulo-cytes for example, contain extended linker stems and have the tendency to fold-back on themselves, forming highly interdigitated structures (Figure 4). Lateral fiber association is also possible *in vivo*, and may explain the absence of distinct chromatin

fibers in many types of nuclei with extensively repressed genomes.[26]

Forces in Biology

Nature and magnitudes

Chemists have been studying intramolecular forces for many years. The importance of forces for the functioning of every living cell has been recognized more recently[50–52] and has led to a sig-nificant research effort to measure them, and to understand how the energy stored in chemical bonds can be transformed into mechanical energy of movement. The processes that involve intra-cellular forces are numerous: the reversible struc-tural transformations of chromatin and chromosomes during the cell cycle, the movements of chromosomes during mitosis and meiosis, of DNA and RNA polymerases along template DNA during replication and transcription, of myosin along actin filaments during muscle contraction, of kinesin along microtubules during vesicle trafficking. Thus, intermolecular forces govern protein–protein and protein–nucleic acid inter-actions, whereas intramolecular forces ensure the proper structuring of biological macromolecules so that they can function properly. The two DNA strands need to be held together in the double-helical structure; RNA molecules have to form the numerous hairpins that define their function; and protein molecules have to fold properly in space to perform whatever function they have.

The magnitude of biologically relevant forces varies within a very broad range (Figure 5). The Langevin (thermal agitation) forces are ubiquitous and random in nature; for objects a couple of microns in size (the dimensions of a typical cell) in water at room temperature, they are in the femtonewton (fN) range. These seemingly minute forces are actually huge in the micro-world: according to Strick *et al.*,[53] a cell experiences a thermal knock equal to its weight every second.

a. 'Tennis-racket' shaped nucleosomes
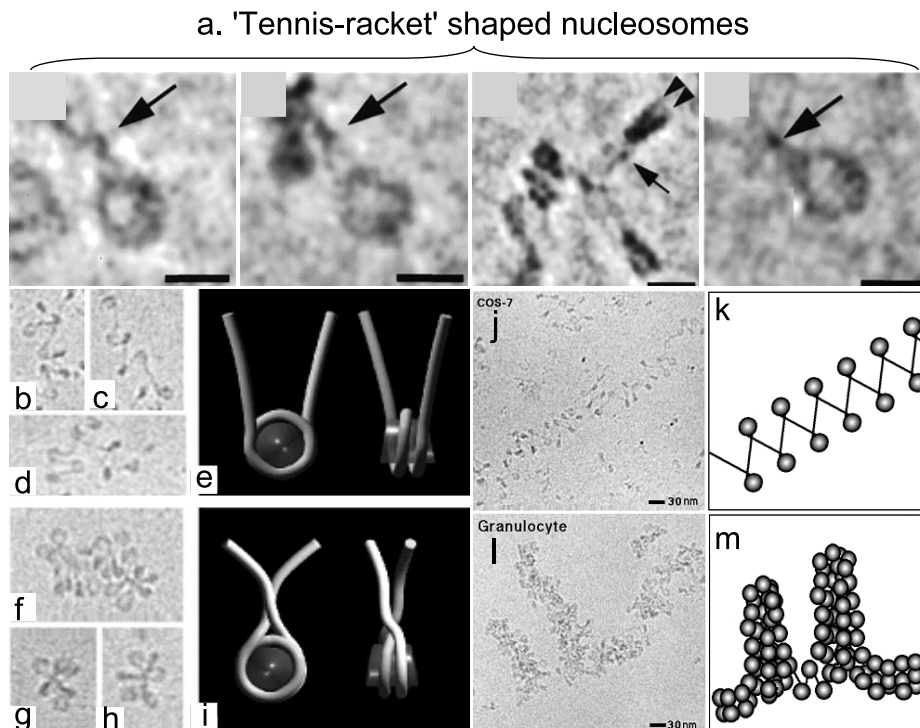
Figure 4. Some example cryo-EM images of chromatin fibers. a, Tennis-racket shaped nucleosomes from Bednar *et al.*[18] Arrows indicate stem structure, and arrowheads show the two DNA gyres around the histone octamer. Copyright (1998) National Academy of Sciences, USA (courtesy of C. Woodcock). b–d, Chromatin fibers from COS-7 cells in a low ionic strength buffer. e, Nucleosome model with diverging linker arms, corresponding to the example images of b–d. f–h, Chromatin fibers, with closely apposed linker DNA stems, from chicken granulocyte cells under similar low ionic strength conditions. i, Nucleosome model with linker arms forming a stem upon exiting, corresponding to the example images of f–h. j, Polynucleosome fibers isolated from COS-7 cells are open 3D zigzag arrangements of nucleosomes. k, Polynucleosome fiber model corresponding to the COS-7 chromatin fiber images. l, Chromatin fibers isolated from differentiated chicken granulocyte cells are highly compact and laterally self-associated. m, Poly-nucleosome fiber model corresponding to the differentiated chicken granulocyte chromatin fiber images. b–m, From Grigoryev[47], with permission of the publisher, courtesy of S. Grigoryev.

The entropic forces within biological macro-molecules, with magnitudes of a few piconewtons, are connected to the reduction of the number of possible configurations accompanying the formation of secondary and tertiary structures. The entropy is maximal when the DNA forms a random coil, or when a protein is denatured: introducing order into these molecules requires work against entropy to be done, and thus depends on the application of force. Forces of the order of a few piconewtons have been experimentally determined upon stretching of DNA in the low force regime (see below). Molecular motors such as myosin, kinesin, and RNA/DNA polymerases develop forces in the same range, from a few piconewtons to tens of piconewtons.[9,54,55]

The forces involved in specific intermolecular interactions (ligand/receptor, antigen/antibody) form the next force magnitude group (Figure 5). When molecular partners interact with each other, many new non-covalent bonds (van der Waals, hydrogen, electrostatic) are created, while many of the pre-existing bonds within each partner are broken to allow a better intermolecular fit. These modifications in the structure of the partners require significant energies, and hence the input of significant forces, usually in the range of 200–300 pN.[14] Similar forces are needed to unfold individually folded domains in polypeptide chains.[56–58] It should be noted that these forces were measured in experiments where the force loading rate, dF/dt, was very high. Experiments that applied the pulling force at much lower loading rate gave lower unfolding forces,[59] in agreement with theoretical considerations on strength of bonds subjected to external force fields.[60,61]

Finally, the forces underlying covalent bonds are almost two orders of magnitude larger than those involved in multi-bond inter- or intramolecular interactions. The phosphodiester bonds in the sugar-phosphate backbone of double-stranded DNA are broken at ~ 1 nN.[54,62,63] Silicon–carbon bonds are ruptured at ~ 2.0 nN, and sulfur–gold bonds break at ~ 1.4 nN.[64]

How interaction forces are measured

The first measurements of intermolecular forces were done with the surface force apparatus (SFA) back in 1973.[65] SFA measures forces between two

macroscopic surfaces as a function of their separation. The distance can be measured with high resolution (1 Å), and the force sensitivity is ∼1 nN. The large contact areas between the surfaces allow only ensemble measurements of forces.

The instruments for measuring forces at the single-molecule level can be divided into two major categories: mechanical force transducers and external field manipulators.[9] In the mechanical force transducers, forces are applied or sensed through the deflections of a bendable beam. In the AFM, it is the flexible cantilever to which the AFM tip is attached that serves as a force transducer/sensor. When the AFM is used to measure forces, the $x-y$ movement of the cantilever is disabled, and it is moved only in the z-direction, upwards and downwards. The deflection of the cantilever is measured as a function of the distance of the tip from the surface, to produce the so-called force curves. A typical AFM force curve is depicted schematically in Figure 6a (with a description in the Figure legend); however, as the reader will see from Figures 7–9, the force curves have a generally similar appearance and are interpreted in similar ways independently of the type of instrument used.

Figure 6b–e exemplify the appearance of force curves in several well understood cases. When there is no specific interaction between the probe (the AFM tip) and the sample, a small blip is seen in the withdrawal curve: the tip stays attached to the sample slightly beyond the point of initial contact upon approach, reflecting the physical adhesion of the tip to the sample (see the legend to Figure 6).[12,14] In the cases of specific interactions (e.g. avidin–biotin, antibody–antigen), this blip turns into a peak, whose magnitude is indicative of the interactive force: the higher the interaction force, the more the cantilever is deflected (see stage 4 in Figure 6a), before it eventually snaps off the sample. If short fragments of double-stranded DNA are stretched, with one strand being attached to the surface and the complementary strand to the tip, the peak changes its shape due to the conformational transition in the double helix before its melting (strand separation). The cantilever deflection measured for a while is less than expected (the peak deviates from a straight line), since the molecule yields to the applied pulling force by stretching beyond its contour length. This overstretching transition has been seen using different stretching approaches but its exact nature is still a point of contention.[15,66]

Finally, when the stretched substrate is a polypeptide chain that contains a number of individually folded domains, the force curves have the saw-tooth appearance presented in Figure 6e.[56–58] The ascending portion of each peak (note the deviation from linearity) corresponds to the entropic stretching of the domain of the polypeptide chain that has unfolded in a preceding peak; at the peak value of force, the domain yields as a whole, abruptly lengthening the molecule
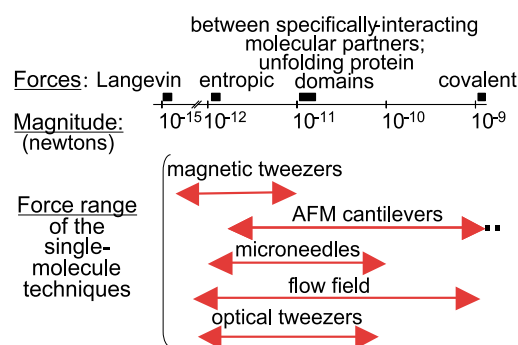

Figure 5. Forces in biology and the force range capabilities of the various single-molecule instruments. The line represents the range of forces encountered in biology, with the filled squares above the line denoting the specific force ranges characteristic of the different types of forces. The arrows below the line illustrate the ranges of forces that can be sensed or applied to biological macromolecules using different techniques.

with a corresponding precipitous drop in the force. The next peak corresponds to unraveling of another domain, and so on, until all domains unfold.

Let us now go back to the instrumentation used for measuring forces. As already stated, the AFM belongs to the category of mechanical force transducers. Other representatives of this category are microneedles and optical fibers to which the manipulated molecule is attached *via* one of its ends (the other end is attached to a bead held by a glass pipette). The bending of these beams is measured in direct microscopic observations[67] or by photodiode detection of light projected from the optical fiber.[68,69]

In the second category of instruments, the external field manipulators, the molecule is acted upon from a distance, by applying external fields: photonic in optical tweezers, magnetic in magnetic tweezers, and hydrodynamic in flow-field apparatuses. The field may be applied to the molecule itself, as is the case of a flow field (see, for example, the chromatin assembly experiments of Ladoux *et al.*,[70] described below, and Figure 11a), or to an appropriate handle to which the molecule is attached (transparent polystyrene beads are used in optical tweezers, whereas beads with magnetic properties are utilized in magnetic tweezers). The other end of the molecule to be manipulated is attached to a surface or an additional bead: this second bead is often held by a micropipette.[71,72]

In optical tweezers,[73] a laser beam is focused through an objective (Figure 1b). A dielectric bead placed in the light path experiences force from multiple photons hitting it: as a photon hits the bead, its momentum changes as a result of the difference in refractive indexes of the medium and the bead; by conservation of momentum, the bead is pushed into a direction opposite to that of the refracted photon. The resultant force from all (refracted and scattered) photons creates a potential
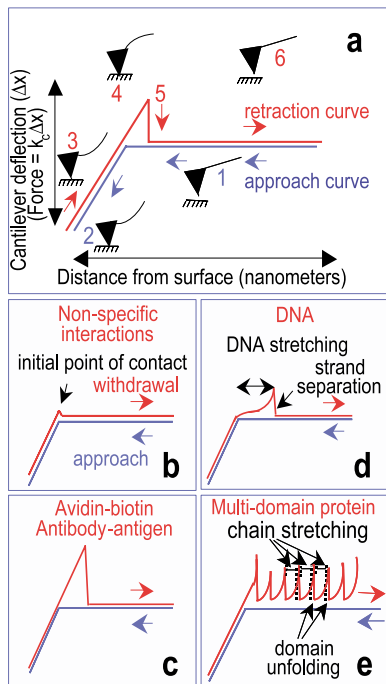
Figure 6. Schematic of a typical force–distance curve recorded by AFM and stylized appearance of force curves reflecting different kinds of interactions.[12,14] a, Explanation of the appearance of a typical force curve. The numbers correspond to different states of the cantilever during the approach and retraction portions of the cycle: (1) AFM tip is not in contact with surface; (2) tip is being pushed into the surface, bending the cantilever; (3) tip is being withdrawn from surface; (4) tip adheres to surface; (5) tip "jumps off contact" from surface; (6) tip is not in contact with surface. b, Non-specific interactions. c, Rupture of bonds between strongly interacting molecular partners, such as avidin–biotin, antibody–antigen. d, DNA stretching force curve. e, Saw-tooth pattern in a force curve obtained upon stretching of multi-domain proteins. For further explanation, see the text.

well slightly below the waist of the beam that holds the bead suspended indefinitely. If a bead is moved out of this equilibrium position (by the application of an external force), it will experience a restoring force that will bring it back to this position. If a macromolecule attached to the bead is pulled or twisted at its other end (e.g. by holding it in a pipette), it will displace the bead from its equilibrium position. Since the force causing the displacement will be counterbalanced by the optical trap, the bead displacement from its equilibrium position can be used to measure the force applied to the molecule.

In magnetic tweezers[53,74−76] force can be applied to a macromolecule tethered between a surface and a paramagnetic bead through the action of an external magnetic field (Figure 1c). The bead, when placed in the magnetic field, acquires a net magnetic moment so that it can now respond to controlled changes in the external field. The distance between the external magnet and the
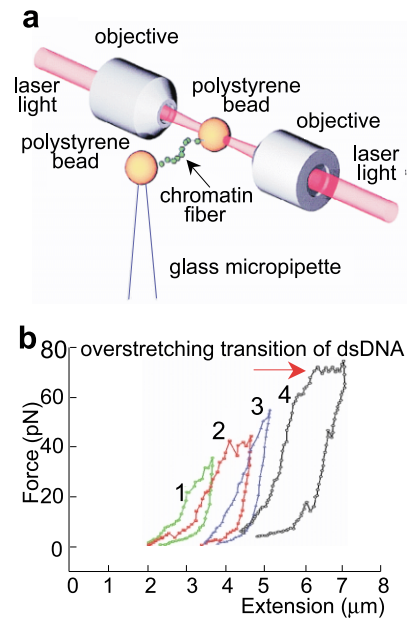
Figure 7. a, Schematic of the experimental approach used by Cui & Bustamante[92] to mechanically stretch isolated chicken erythrocyte chromatin fibers. b, Force curves obtained in consecutive stretch-relaxation cycles (redrawn from Cui & Bustamante).[92]
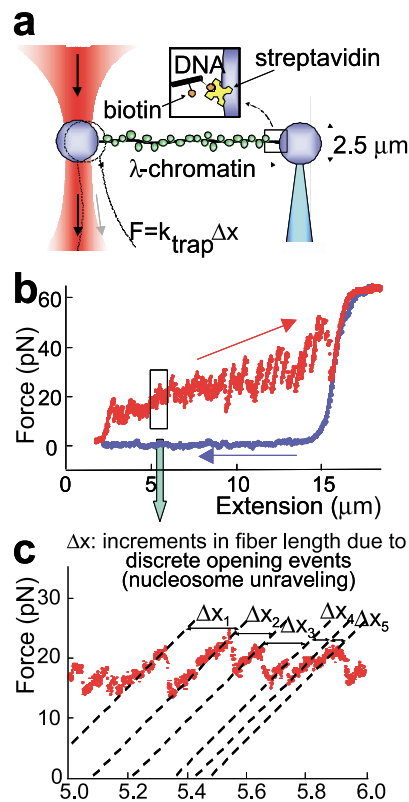
Figure 8. a, Schematic of the experimental approach used by Bennink *et al.*[72] to mechanically stretch chromatin fibers directly assembled in the flow cell from a single λ DNA molecule and *Xenopus* cell-free extracts. b, A representative force curve. c, A blow-up of the boxed region of the curve in b. For further explanation, see the text.
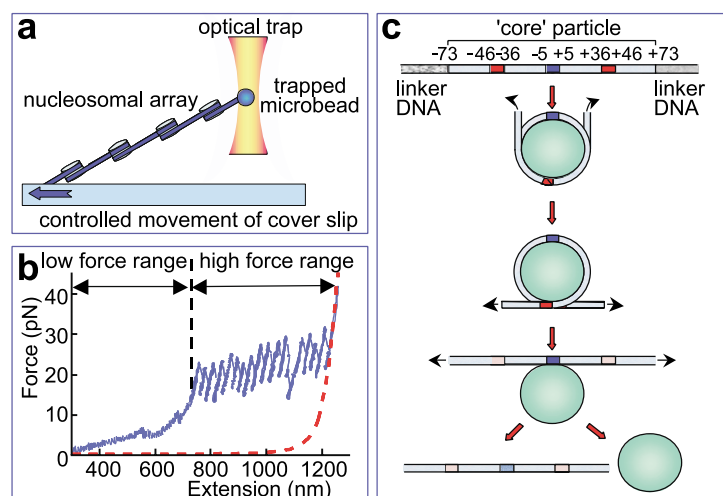
Figure 9. a, Schematic of the experimental approach used by Brower-Toland *et al.*[93] to mechanically stretch pre-assembled, fully saturated nucleosomal arrays containing 17 positioned nucleosomes. b, A force curve obtained upon moving the coverslip at a constant velocity relative to the bead, whose position was kept constant by modulating the light intensity of the trapping laser (velocity clamp mode of operation); the low force range and high force range are designated, with discrete opening events seen only in the high force range. c, The suggested three-stage model for the mechanical disruption of the nucleosomal particle (redrawn or modified from Brower-Toland *et al.*[93]).

bead controls the magnitude of force applied to the molecule. Moreover, the alignment of the acquired magnetic moment of the bead with the external field allows controlled rotation of the bead, in synchrony with a controlled rotation of the external magnet(s). This rotation allows the application of a controlled torque to the molecule suspended between the bead and the surface, given that the molecule is attached in a topologically constrained way so that it cannot swivel about its anchoring points. Thus, in a series of experiments, the laboratory of David Bensimon and Vincent Croquette[75,77,78] was able to introduce controlled positive or negative supercoiling in DNA molecules attached to the surfaces *via* multiple contacts on all four ends. By recording force-extension curves at fixed values of superhelical density and constant forces (ranging from 6 fN to 20 pN) and replotting the data as extension-superhelical density curves, the authors revealed intriguing differences in the behavior of positively *versus* negatively supercoiled molecules, at intermediate and high forces. At intermediate forces (~ 1.2 pN), the negatively supercoiled molecules did not form plectonemes upon pumping of superhelicity; instead, the torsional stress was absorbed by local denaturation. In the high force regime (> 3 pN), no plectoneme formation was observed for either negatively or positively supercoiled DNA; the positively supercoiled DNA underwent a transition to a new structure (called P-DNA, for Pauling-DNA), in which the phosphate-sugar backbone is winding inside the structure and the bases are exposed to the solution. The same group applied magnetic tweezers to study the action of several topoisomerases.[79–81]

In flow field experiments, the flow force can be applied either directly to the molecule or through a bead handle. The forces are estimated using Stokes' law, which requires precise knowledge of flow rates. The main advantages of the flow field

approach lie in the wide range of forces that can be readily applied and the ease of changing buffers and biofactors needed for particular biochemical reactions to take place (for further details on this technique, see Bustamante *et al.*[9]).

Figure 5 schematically presents the range of forces that can be applied by the different single-molecule manipulation techniques.

Chromatin disassembly under applied force

DNA was the first biological macromolecule to be studied under applied force. Fragments of DNA several micrometers long have been stretched by a combination of magnetic and flow forces,[74] optical tweezers,[71,82] glass needles/optical fibers,[68,83] and AFM[84,85] (AFM has been also used to stretch short double-stranded oligonucleotides).[86,87] In general, the DNA molecule behaves in a different way under different force regimes.[15,54,66] Under tensile forces of up to ~ 10 pN, DNA behaves as an elastic rod, accurately described by an inextensible worm-like chain model. This purely entropic behavior changes above 10 pN, when the molecule lengthens beyond its *B*-form contour length, i.e. it behaves as a stretchable solid with a certain elastic stretch modulus. This stretching must result from changing of the chemical structure itself in response to the relatively high tensile force applied. When the force exceeds ~ 65 pN, the molecule suddenly yields and overstretches to ~ 1.7 times its contour length (the overstretching force plateau occurs at 110 pN for dsDNA molecules not containing nicks[83]). The overstretching transition force is a function of the salt concentration,[82] and is highly sequence-dependent.[84] The force rises rapidly again following the overstretching transition, to reach a new smaller plateau at

~ 150 pN, after which the force curve for dsDNA overlies the force curve for ssDNA. The exact nature of the structural transformations during the different stages of stretching remains controversial, with the possible exception of the very first entropic stage and the very last stage where complete melting of the helix seems to occur (for a detailed discussion, see Zlatanova & Leuba[15]).

Attempts to mechanically stretch chromatin fibers have considerably lagged behind such studies on naked DNA. The initial attempts used AFM to stretch both isolated native fibers and reconstituted nucleosomal arrays.[88,89] The force-extension curves had the multi-peak, saw-tooth pattern expected to be seen as a result of consecutive disassembly of individual nucleosomes in the fiber: the unraveling of the DNA from around each histone octamer was expected to lengthen the fiber in a jump, to be accompanied by an abrupt drop in the force (this expectation was based on the known behavior of multi-domain proteins subjected to stretching;[90,91] see Figure 6e). Careful analysis of the force curves, however, suggested that the force jumps corresponded to removal of successive intact nucleosomes from the glass surface, followed by stretching of the naked DNA between the nucleosomes attached to the tip and the surface. The surface attachment artifact could be, in principle, overcome by suspending the chromatin fiber between the AFM tip and the surface; however, such experiments have not been reported.

Single chromatin fibers have been successfully stretched with optical tweezers. Cui and Bustamante[92] used a dual-beam optical trap to pull on isolated chicken erythrocyte chromatin fibers suspended between the trapped bead and a bead held by a glass micropipette (Figure 7a). The force curves showed that up to 20 pN the fibers underwent reversible stretching, whereas application of forces above this value led to irreversible alterations interpreted in terms of histone dissociation, with recovery of the mechanical properties of naked DNA (Figure 7b).

The optical tweezers set-up used by Bennink *et al.*[72] was quite similar (Figure 8a), but the experimental approach was different. Rather than using chromatin fibers isolated from cells (by definition these fibers are somewhat heterogeneous in length and may also be compositionally heterogeneous depending on which part of the genome they originate from), these authors resorted to assembling the nucleosomal arrays to be stretched directly in the flow cell. To that end, a single λ DNA molecule was attached *via* its biotinylated 5′ ends to streptavidin-coated beads, and nucleosome assembly was carried out by flowing in cell-free *Xenopus* extracts that contained core histones and the protein assembly factors needed for proper nucleosome formation. The transformation of the naked DNA into a chromatin fiber was followed by the shortening of the distance between the pipette-held bead and the "free" bead attached to the

other end of the DNA molecule (technical considerations demanded the use of the optical trap to be discontinued during the assembly step, to be again turned on during the stretching phase; see more below). Once the chromatin fiber was assembled, it was stretched by moving the pipette away from the trapped bead and force-extension curves were recorded. The high speed of data acquisition in these experiments resulted in force curves with a large number of easily discernible, discrete peaks (Figure 8b and c). Each peak reflects the opening (unraveling) of an individual nucleosome (or small groups of two, three or four nucleosomes), as judged by the increments in fiber length from one stretching intermediate to the next (see Figure 8c for illustration of this measurement). The fiber lengthens in increments of ~ 65 nm or multiples thereof (see Figure 4 of Bennink *et al.*,[72] for the original analysis), that roughly correspond to the change in fiber length as a result of unwrapping of two full turns of the DNA superhelix from around the histone octamer. Importantly, the forces required to break the histone/DNA bonds are in the range between 20 pN and 40 pN, in agreement with the data of Cui & Bustamante.[92]

Recently, the laboratory of M. Wang reported another optical tweezers study, in which a nucleosomal array containing 17 positioned nucleosomes on an artificial DNA construct was assembled in solution, and then attached to a bead in an optical trap and to a coverslip; the array was stretched by controlled movement of the coverslip[93] (Figure 9a). Analysis of the force-extension curves suggested that approximately one half of each nucleosome was disrupted at low forces (with no characteristic discrete, single-nucleosome signature identified in this force regime), while the remaining half unraveled at forces exceeding 20 pN, with each nucleosome giving an individual peak in the force curve. Such a step-wise unraveling process would be possible if the nucleosomal particle structure were held together by histone–DNA interactions of rather different strengths at different locations along the DNA. Indeed, such variability in contact strength along the length of the core particle DNA has been inferred from the crystal structure, with the weakest interactions occurring at the ends, and the strongest interactions occurring at the dyad axis.[6,94] This pattern of differential strength of histone–DNA interactions along the core particle DNA may be the structural basis for the dynamic "breathing" of the DNA ends,[7] to give the nucleosomal particle the flexibility needed for its proper functioning.[95] The step-wise model for nucleosome unraveling is illustrated in Figure 9c. It should be noted that although the model suggests simultaneous unraveling of both ends of the nucleosomal DNA until the relatively strong contacts at positions $+4$ and -4 of the DNA superhelix are reached, an alternative step-wise model may be conceivable, in which one half of the particle unravels unilaterally, with the strong contacts at the dyad serving as a roadblock to a

total quick release of the entire DNA from the histone surface (J. Widom, personal communication). In this scenario, the release of the first half may occur gradually (to concur with the lack of discrete lengthening peaks in the low force regime), whereas the second half of each nucleosome may be released in a jump, following the rupture of the contacts at the dyad (to explain the discrete peaks in the high force regime).

Thus, the opening events described by Bennink et al.[72] would correspond to unraveling of the entire particle at once (~65 nm steps), while the discernible opening events described by Brower-Toland et al.[93] would correspond only to the second phase of the DNA unwrapping from around the histone core (~27 nm). Understanding the reason for this different behavior of the nucleosomal particle will require additional studies (now in progress in our laboratories). Importantly though, all three reports agree on the magnitude of forces required to unravel nucleosomes, ~20–40 pN.

What may the physiological relevance of these results be? It turns out that the forces measured for RNA and DNA polymerases[96–99] are in exactly the same range as those keeping the integrity of the nucleosomal particle. Can it then be postulated that the DNA-tracking enzymes may be capable of clearing nucleosomes out of their way by themselves, without the help of auxiliary factors? Before jumping to conclusions, it is important to note that the enzymes used in these studies are of prokaryotic or phage origin, i.e. they never encounter nucleosomes in their physiological environment. On the other hand, though, recent high-resolution crystal structures of a phage polymerase (T7),[100,101] a bacterial enzyme (*Thermus aquaticus*)[102] and a eukaryotic Pol II (yeast)[103,104] show an amazing degree of evolutionary conservation of structure, especially in and around the active centers in the catalytic subunits. These structural similarities, together with the numerous shared functional characteristics,[105–108] make it rather probable that the forces that are exerted by the enzymes on the DNA threaded through their active centers are of similar magnitudes.

Finally, it is instructive to directly compare the behavior of naked DNA with that of chromatin fibers stretched under identical conditions. As Figure 10 indicates, the force-relative extension curves for λ DNA and λ chromatin are quite different, and so are the numerical values for the persistence length and stretch modulus extracted from these curves. The molecular features of the two stretching substrates that give rise to these differences are difficult to assess at present.

Chromatin assembly under applied force

Studying nucleosomal strength and the forces needed to break down the nucleosome is obviously an important, physiologically relevant issue. What
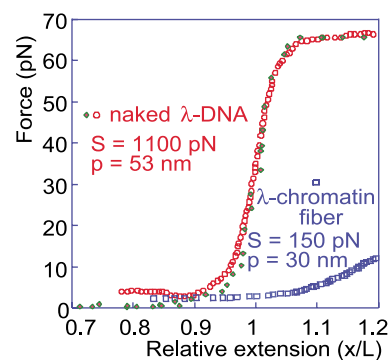
Figure 10. Comparison of naked λ DNA and λ-chromatin fiber stretch curves. Naked DNA force-relative extension curve redrawn from Bustamante et al.[54] (diamonds) or plotted from the data of Bennink et al.[72] (circles) using a contour length for the stretched λ DNA of 16 μm. The force-relative extension curve of the λ chromatin fiber (squares) was calculated from the data of the completely reversible portion of the stretch curve in the low force regime (see 2–3 μm portion in Figure 8b), using a contour length of 2.3 μm (determined as the *x*-intercept of a linear fit to the data). The numerical values for the stretch modulus (*S*) and the persistence length (*P*) for both naked λ DNA and λ chromatin fiber are listed in the graph.

about studying chromatin assembly under applied force? Chromatin assembly *in vivo* takes place massively at the newly formed double helices, immediately following DNA replication. Nucleosomes have to assemble also in the wake of the transcriptional machinery, since the mechanism of DNA transcription requires temporal removal of all proteins bound to the template DNA, including the histones of the core particle. The upstream (already transcribed) naked DNA stretches that emerge from the polymerase must, within a reasonable time, recover their chromatin structure to allow resumption of the roles chromatin plays in DNA compaction and regulation of its function. This reformation of nucleosomes in the wake of RNA polymerase (and, for that matter, of other DNA-tracking enzymes as well) occurs while the DNA molecule is still under tension as a result of the pulling exerted by the stationary polymerase on the transcribed DNA. As already alluded to, polymerases are *bona fide* molecular motors developing pretty high forces (up to 30–40 pN).[97,98] If the forces measured *in vitro* are physiologically relevant, then it is important to understand how and under what conditions nucleosomes assemble, i.e. what the force dependence of the assembly process is.

Three laboratories have approached this issue at the single-molecule level. Viovy and his co-workers followed chromatin formation in real time by recording the shortening of a single λ DNA molecule attached to a glass surface, and subjected to defined flow fields[70] (Figure 11a). The
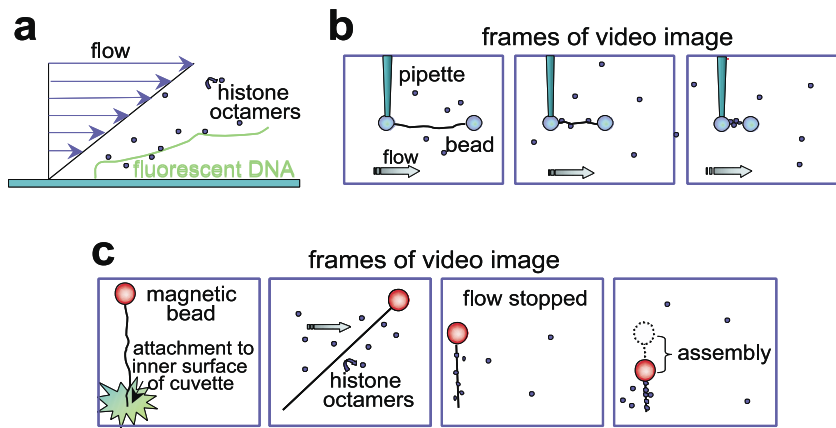
Figure 11. Schematics of methods applied to study the force dependence of nucleosome assembly on long single DNA molecules using: a, flow;[70] b, optical tweezers/flow;[109] c, magnetic tweezers/flow.[110]

molecule was fluorescently labeled by intercalation of YOYO-1, and chromatin assembly was achieved by flowing in *Xenopus* or *Drosophila* cell-free extracts. Bennink *et al.*[109] used a similar biological system (λ DNA and *Xenopus* extracts) in an optical trap/flow field set-up (Figure 11b). The optical trap was used for the initial attachment of the single DNA molecule between two beads, but was subsequently turned off during the assembly (the presence of cell debris in the extract precluded the use of the optical trap for force measurements). Forces were applied *via* the flow field, and were estimated either by Stokes' law or by measurement of the Brownian motion of the freely suspended bead. Finally, Leuba *et al.*[110] used magnetic tweezers to study the force dependence of chromatin

assembly in an approach depicted in Figure 11c. Nucleosomes were formed on λ DNA molecules suspended between a paramagnetic bead and the inner surface of a glass cuvette by the addition of purified histone octamers and recombinant nucleosome assembly protein 1 (NAP-1). Once the shortening of DNA became visible, the flow was stopped, and assembly was performed only under the magnetic force. All three groups reported qualitatively similar results; we will illustrate them by the example of the magnetic tweezers approach.

Curves of the travel of the bead across the video-screen as a function of time were first recorded at a constant force (for a representative curve, see Figure 12a). From each of these curves, we
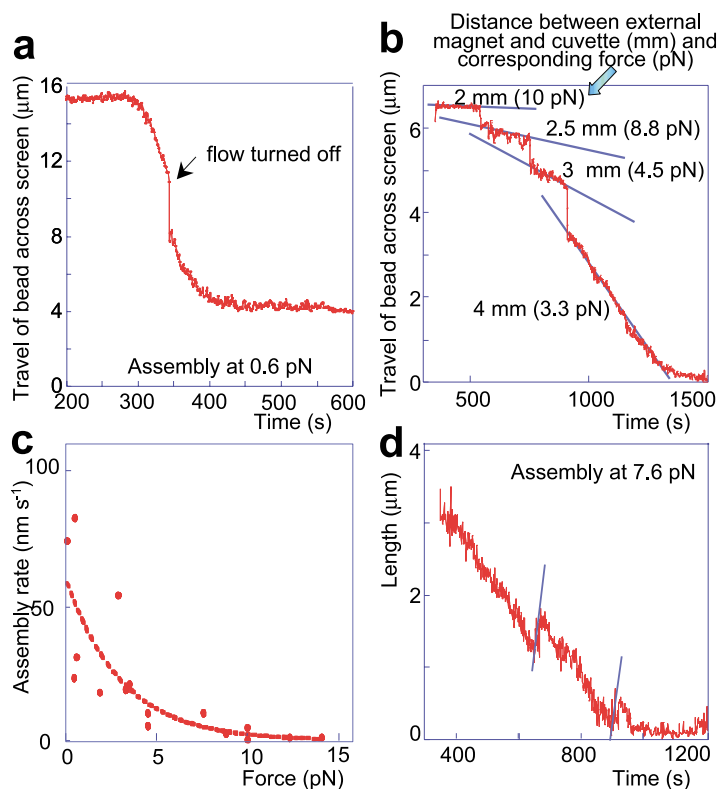
Figure 12. Example of experimental data on chromatin assembly with magnetic tweezers.[110] a, Raw assembly curve recorded at 0.6 pN in a flow-stopped experiment. b, A rheostat experiment, with step-wise changes of the distance between the external magnet and the cuvette, hence of the force applied to the magnetic bead. c, Data from 18 individual assembly experiments performed at different forces: each point is the initial assembly rate at a given force. The dotted curve is an exponential fit to the data. d, An assembly curve recorded at 7.6 pN. Note the upward steps on the otherwise descending curve. These steps appear as a result of the dynamic equilibrium between nucleosome assembly and disassembly (for further details, see the text, and Leuba *et al.*[110]).

estimated the initial assembly rate at the specified force. In addition, we performed "rheostat" experiments in which the force applied to the bead, and hence to the DNA molecule, was changed stepwise during the course of a single assembly experiment. This rheostat control over the force was easily achieved through changing the distance between the external magnet and the cuvette (hence the bead). An assembly curve recorded in such an experiment is illustrated in Figure 12b; it shows clearly that the assembly rate is dependent on the applied force: the higher the force, the slower the assembly. Importantly, it also indicates that the response of the system to changes in force is instantaneous. Figure 12c is a plot of the data from many individual experiments and shows, in agreement with the previous reports, that forces around 10 pN effectively prevent nucleosome formation. It remains to be seen how the forces "stalling" nucleosome formation are related to the forces developed by the transcriptional machinery as a function of the rate of transcription.

One last point from these experiments deserves mentioning. A careful look at the portion of the assembly curve presented in Figure 12d reveals upward jumps on the otherwise monotonous downward assembly curve. Such jumps are more frequent in curves recorded at higher forces and must reflect occasional spontaneous disassembly of nucleosomes (probably several at a time). This is the first real-time demonstration of the dynamic equilibrium between nucleosome formation and dissociation in the fiber context; the existence of such equilibrium at the mononucleosome level has been previously suggested from bulk experiments and theory.[1,111]

It should be noted that all three assembly studies made use of DNA molecules that were not topologically constrained, i.e. were free to swivel around their attachment points. It is obviously necessary to study the force dependence of nucleosome assembly on topologically constrained DNA molecules, to more closely mimic the *in vivo* situation of chromatin fibers organized in loops attached to components of the nuclear matrix.

What's next?

The brief description of the single-molecule studies in the chromatin field may leave the reader with mixed feelings. Intriguing, maybe enchanting, but is this all? Is this just another example of "much ado about nothing"? What other questions can be approached? What other techniques can be used? We believe that the possibilities are endless. Think of any system, any process you want to study. Is there a better way to really understand what is going on than looking at one molecule/molecular complex at a time, so that crucial characteristics are not lost, masked by the average measurements of huge populations of molecules? Is there a better way to follow the kinetics of

intrinsically asynchronous processes, like transcription, for example, where synchrony is quickly lost even if you initiate the biochemical reaction in a synchronized molecular population? Think about the complexities of transcription through nucleosomes superimposed on the complexities of transcription on naked DNA templates. Think about how much we can learn if we could transcribe individual nucleosomes one-at-a-time, for example. What about understanding replication, repair, recombination in the chromatin context?

We believe that the single-molecule chromatin field is just making its first steps. Still, the power of the single-molecule techniques in approaching important structural and functional chromatin issues cannot be overstated. The chromatin research community will need to embrace these techniques wholeheartedly, in the realization that only by combining the new single-molecule tools with the more traditional biochemical and biophysical approaches can we hope to achieve any major breakthrough in our understanding of chromatin structure and function. The future is thrilling and bright, though not necessarily easy.

References

1. van Holde, K. E. (1988). *Chromatin*, Springer Series in Molecular Biology, Springer, New York.
2. Tsanev, R., Russev, G., Pashev, I. & Zlatanova, J. (1992). *Replication and Transcription of Chromatin*, CRC Press, Boca Raton.
3. Wolffe, A. P. (1998). *Chromatin: Structure and Function*, Academic Press, New York.
4. Turner, B. M. (2002). *Chromatin and Gene Regulation: Mechanisms in Epigenetics*, Blackwell Science, Oxford.
5. Arents, G. & Moudrianakis, E. N. (1993). Topography of the histone octamer surface: repeating structural motifs utilized in the docking of nucleosomal DNA. *Proc. Natl Acad. Sci. USA*, **90**, 10489–10493.
6. Luger, K., Mader, A. W., Richmond, R. K., Sargent, D. F. & Richmond, T. J. (1997). Crystal structure of the nucleosome core particle at 2.8 Å resolution. *Nature*, **389**, 251–260.
7. van Holde, K. & Zlatanova, J. (1999). The nucleosome core particle: does it have structural and physiologic relevance? *Bioessays*, **21**, 776–780.
8. Harp, J. M., Hanson, B. L., Timm, D. E. & Bunick, G. J. (2000). Asymmetries in the nucleosome core particle at 2.5 Å resolution. *Acta Crystallog. sect. D*, **56**, 1513–1534.

9. Bustamante, C., Macosko, J. C. & Wuite, G. J. (2000). Grabbing the cat by the tail: manipulating molecules one by one. *Nature Rev. Mol. Cell Biol.* **1**, 130–136.

10. Leuba, S. H.; Zlatanova, J. (eds) (2001). Biology at the single-molecule level., Amsterdam, Pergamon.

11. Binnig, G., Quate, C. F. & Rohrer, C. (1986). Atomic force microscope. *Phys. Rev. Letters*, **56**, 930–933.

12. Cappella, B. & Dietler, G. (1999). Force–distance curves by atomic force microscopy. *Surf. Sci. Rep.* **34**, 1–104.

13. Heinz, W. F. & Hoh, J. H. (1999). Spatially resolved force spectroscopy of biological surfaces using the atomic force microscope. *Trends Biotechnol.* **17**, 143–150.

14. Zlatanova, J., Lindsay, S. M. & Leuba, S. H. (2000). Single molecule force spectroscopy in biology using the atomic force microscope. *Prog. Biophys. Mol. Biol.* **74**, 37–61.

15. Zlatanova, J. & Leuba, S. H. (2002). Stretching and imaging single DNA molecules and chromatin. *J. Muscle Res. Cell Motil.*, 23.

16. Zlatanova, J. & Leuba, S. H. (2003). Chromatin structure and dynamics: lessons from single molecule approaches. In *Chromatin Structure and Dynamics: State-of-the-Art* (Zlatanova, J. & Leuba, S. H., eds), Elsevier, Amsterdam.

17. Bednar, J., Horowitz, R. A., Dubochet, J. & Woodcock, C. L. (1995). Chromatin conformation and salt-induced compaction: three-dimensional structural information from cryoelectron microscopy. *J. Cell Biol.* **131**, 1365–1376.

18. Bednar, J., Horowitz, R. A., Grigoryev, S. A., Carruthers, L. M., Hansen, J. C., Koster, A. J. & Woodcock, C. L. (1998). Nucleosomes, linker DNA, and linker histone form a unique structural motif that directs the higher-order folding and compaction of chromatin. *Proc. Natl Acad. Sci. USA*, **95**, 14173–14178.

19. Woodcock, C. L., Grigoryev, S. A., Horowitz, R. A. & Whitaker, N. (1993). A chromatin folding model that incorporates linker variability generates fibers resembling the native structures. *Proc. Natl Acad. Sci. USA*, **90**, 9021–9025.

20. Leuba, S. H., Yang, G., Robert, C., Samori, B., van Holde, K., Zlatanova, J. & Bustamante, C. (1994). Three-dimensional structure of extended chromatin fibers as revealed by tapping-mode scanning force microscopy. *Proc. Natl Acad. Sci. USA*, **91**, 11621–11625.

21. Yang, G., Leuba, S. H., Bustamante, C., Zlatanova, J. & van Holde, K. (1994). Role of linker histones in extended chromatin fibre structure. *Nature Struct. Biol.* **1**, 761–763.

22. van Holde, K. & Zlatanova, J. (1995). Chromatin higher order structure: chasing a mirage? *J. Biol. Chem.* **270**, 8373–8376.

23. Finch, J. T. & Klug, A. (1976). Solenoidal model for superstructure in chromatin. *Proc. Natl Acad. Sci. USA*, **73**, 1897–1901.

24. Thoma, F., Koller, T. & Klug, A. (1979). Involvement of histone H1 in the organization of the nucleosome and of the salt-dependent superstructures of chromatin. *J. Cell Biol.* **83**, 403–427.

25. van Holde, K. & Zlatanova, J. (1996). What determines the folding of the chromatin fiber? *Proc. Natl Acad. Sci. USA*, **93**, 10548–10555.

26. Woodcock, C. L. & Horowitz, R. A. (1995). Chroma-tin organization re-viewed. *Trends Cell Biol.* **5**, 272–277.

27. Zlatanova, J., Leuba, S. H. & van Holde, K. (1998). Chromatin fiber structure: morphology, molecular determinants, structural transitions. *Biophys. J.* **74**, 2554–2566.

28. Zlatanova, J., Leuba, S. H. & van Holde, K. (1999). Chromatin structure revisited. *Crit. Rev. Eukaryot. Gene Expr.* **9**, 245–255.

29. Leuba, S. H., Bustamante, C., van Holde, K. & Zlatanova, J. (1998). Linker histone tails and N-tails of histone H3 are redundant: scanning force microscopy studies of reconstituted fibers. *Biophys. J.* **74**, 2830–2839.

30. Leuba, S. H., Bustamante, C., Zlatanova, J. & van Holde, K. (1998). Contributions of linker histones and histone H3 to chromatin structure: scanning force microscopy studies on trypsinized fibers. *Biophys. J.* **74**, 2823–2829.

31. Schnitzler, G. R., Cheung, C. L., Hafner, J. H., Saurin, A. J., Kingston, R. E. & Lieber, C. M. (2001). Direct imaging of human SWI/SNF-remodeled mono- and polynucleosomes by atomic force microscopy employing carbon nanotube tips. *Mol. Cell Biol.* **21**, 8504–8511.

32. Karymov, M. A., Tomschik, M., Leuba, S. H., Caiafa, P. & Zlatanova, J. (2001). DNA methylation-dependent chromatin fiber compaction *in vivo* and *in vitro*: requirement for linker histone. *FASEB J.* **15**, 2631–2641.

33. An, W., Palhan, V. B., Karymov, M. A., Leuba, S. H. & Roeder, R. G. (2002). Selective requirements for histone H3 and H4 N termini in p300-dependent transcriptional activation from chromatin. *Mol. Cell*, **9**, 811–821.

34. Martin, L. D., Vesenka, J. P., Henderson, E. & Dobbs, D. L. (1995). Visualization of nucleosomal sub-structure in native chromatin by atomic force microscopy. *Biochemistry*, **34**, 4610–4616.

35. Zhao, H., Zhang, Y., Zhang, S. B., Jiang, C., He, Q. Y., Li, M. Q. & Qian, R. L. (1999). The structure of the nucleosome core particle of chromatin in chicken erythrocytes visualized by using atomic force microscopy. *Cell Res.* **9**, 255–260.

36. Shao, Z. (1999). Probing nanometer structures with atomic force microscopy. *News Physiol. Sci.* **14**, 142–149.

37. Sato, M. H., Ura, K., Hohmura, K. I., Tokumasu, F., Yoshimura, S. H., Hanaoka, F. & Takeyasu, K. (1999). Atomic force microscopy sees nucleosome positioning and histone H1-induced compaction in reconstituted chromatin. *FEBS Letters*, **452**, 267–271.

38. Dubochet, J., Adrian, M., Dustin, I., Furrer, P. & Stasiak, A. (1992). Cryoelectron microscopy of DNA molecules in solution. *Methods Enzymol.* **211**, 507–518.

39. Dubochet, J. (1993). Twisting in a crowd. *Trends Cell Biol.* **3**, 1–3.

40. Bednar, J. & Woodcock, C. L. (1999). Cryoelectron microscopic analysis of nucleosomes and chroma-tin. *Methods Enzymol.* **304**, 191–213.

41. Dubochet, J., Adrian, M., Schultz, P. & Oudet, P. (1986). Cryo-electron microscopy of vitrified SV40 minichromosomes: the liquid drop model. *EMBO J.* **5**, 519–528.

42. Ehrlich, L., Munkel, C., Chirico, G. & Langowski, J. (1997). A Brownian dynamics model for the chromatin fiber. *Comput. Appl. Biosci.* **13**, 271–279.

43. Katritch, V., Bustamante, C. & Olson, W. K. (2000).

Pulling chromatin fibers: computer simulations of direct physical micromanipulations. *J. Mol. Biol.* **295**, 29–40.

44. Hammermann, M., Toth, K., Rodemer, C., Waldeck, W., May, R. P. & Langowski, J. (2000). Salt-dependent compaction of di- and trinucleosomes studied by small-angle neutron scattering. *Biophys. J.* **79**, 584–594.

45. Schiessel, H., Gelbart, W. M. & Bruinsma, R. (2001). DNA folding: structural and mechanical properties of the two-angle model for chromatin. *Biophys. J.* **80**, 1940–1956.

46. Wedemann, G. & Langowski, J. (2002). Computer simulation of the 30-nanometer chromatin fiber. *Biophys. J.* **82**, 2847–2859.

47. Grigoryev, S. A. (2001). Higher-order folding of heterochromatin: protein bridges span the nucleosome arrays. *Biochem. Cell Biol.* **79**, 227–241.

48. Hamiche, A., Schultz, P., Ramakrishnan, V., Oudet, P. & Prunell, A. (1996). Linker histone-dependent DNA structure in linear mononucleosomes. *J. Mol. Biol.* **257**, 30–42.

49. Grigoryev, S. A., Bednar, J. & Woodcock, C. L. (1999). MENT, a heterochromatin protein that mediates higher order chromatin folding, is a new serpin family member. *J. Biol. Chem.* **274**, 5626–5636.

50. Khan, S. & Sheetz, M. P. (1997). Force effects on biochemical kinetics. *Annu. Rev. Biochem.* **66**, 785–805.

51. Leckband, D. (2000). Measuring the forces that control protein interactions. *Annu. Rev. Biophys. Biomol. Struct.* **29**, 1–26.

52. Leckband, D. & Israelachvili, J. (2001). Intermolecular forces in biology. *Quart. Rev. Biophys.* **34**, 105–267.

53. Strick, T. R., Allemand, J. F., Bensimon, D. & Croquette, V. (2000). Stress-induced structural transitions in DNA and proteins. *Annu. Rev. Biophys. Biomol. Struct.* **29**, 523–543.

54. Bustamante, C., Smith, S. B., Liphardt, J. & Smith, D. (2000). Single-molecule studies of DNA mechanics. *Curr. Opin. Struct. Biol.* **10**, 279–285.

55. Thomas, N., Imafuku, Y., Kamiya, T. & Tawada, K. (2002). Kinesin: a molecular motor with a spring in its step. *Proc. Roy. Soc. ser. B*, **269**, 2363–2371.

56. Clausen-Schaumann, H., Seitz, M., Krautbauer, R. & Gaub, H. E. (2000). Force spectroscopy with single bio-molecules. *Curr. Opin. Chem. Biol.* **4**, 524–530.

57. Fisher, T. E., Oberhauser, A. F., Carrion-Vazquez, M., Marszalek, P. E. & Fernandez, J. M. (1999). The study of protein mechanics with the atomic force microscope. *Trends Biochem. Sci.* **24**, 379–384.

58. Carrion-Vazquez, M., Oberhauser, A. F., Fisher, T. E., Marszalek, P. E., Li, H. & Fernandez, J. M. (2000). Mechanical design of proteins studied by single-molecule force spectroscopy and protein engineering. *Prog. Biophys. Mol. Biol.* **74**, 63–91.

59. Merkel, R., Nassoy, P., Leung, A., Ritchie, K. & Evans, E. (1999). Energy landscapes of receptor–ligand bonds explored with dynamic force spectroscopy. *Nature*, **397**, 50–53.

60. Evans, E. & Ritchie, K. (1997). Dynamic strength of molecular adhesion bonds. *Biophys. J.* **72**, 1541–1555.

61. Evans, E. (2001). Probing the relation between force–lifetime–and chemistry in single molecular bonds. *Annu. Rev. Biophys. Biomol. Struct.* **30**, 105–128.

62. Bensimon, A., Simon, A., Chiffaudel, A., Croquette, V., Heslot, F. & Bensimon, D. (1994). Alignment and sensitive detection of DNA by a moving interface. *Science*, **265**, 2096–2098.

63. Bensimon, D., Simon, A. J., Croquette, V. V. & Bensimon, A. (1995). Stretching DNA with a receding meniscus: experiments and models. *Phys. Rev. Letters*, **74**, 4754–4757.

64. Grandbois, M., Beyer, M., Rief, M., Clausen-Schaumann, H. & Gaub, H. E. (1999). How strong is a covalent bond? *Science*, **283**, 1727–1730.

65. Israelachvili, J. N. (1992). *Intermolecular and Surface Forces*, Academic Press, New York.

66. Williams, M. C. & Rouzina, I. (2002). Force spectroscopy of single DNA and RNA molecules. *Curr. Opin. Struct. Biol.* **12**, 330–336.

67. Kishino, A. & Yanagida, T. (1988). Force measurements by micromanipulation of a single actin filament by glass needles. *Nature*, **334**, 74–76.

68. Cluzel, P., Lebrun, A., Heller, C., Lavery, R., Viovy, J. L., Chatenay, D. & Caron, F. (1996). DNA: an extensible molecule. *Science*, **271**, 792–794.

69. Leger, J. F., Robert, J., Bourdieu, L., Chatenay, D. & Marko, J. F. (1998). RecA binding to a single double-stranded DNA molecule: a possible role of DNA conformational fluctuations. *Proc. Natl Acad. Sci. USA*, **95**, 12295–12299.

70. Ladoux, B., Quivy, J. P., Doyle, P., du Roure, O., Almouzni, G. & Viovy, J. L. (2000). Fast kinetics of chromatin assembly revealed by single-molecule videomicroscopy and scanning force microscopy. *Proc. Natl Acad. Sci. USA*, **97**, 14251–14256.

71. Smith, S. B., Cui, Y. & Bustamante, C. (1996). Overstretching B-DNA: the elastic response of individual double-stranded and single-stranded DNA molecules. *Science*, **271**, 795–799.

72. Bennink, M. L., Leuba, S. H., Leno, G. H., Zlatanova, J., de Grooth, B. G. & Greve, J. (2001). Unfolding individual nucleosomes by stretching single chromatin fibers with optical tweezers. *Nature Struct. Biol.* **8**, 606–610.

73. Ashkin, A. (1997). Optical trapping and manipulation of neutral particles using lasers. *Proc. Natl Acad. Sci. USA*, **94**, 4853–4860.

74. Smith, S. B., Finzi, L. & Bustamante, C. (1992). Direct mechanical measurements of the elasticity of single DNA molecules by using magnetic beads. *Science*, **258**, 1122–1126.

75. Strick, T. R., Allemand, J. F., Bensimon, D., Bensimon, A. & Croquette, V. (1996). The elasticity of a single supercoiled DNA molecule. *Science*, **271**, 1835–1837.

76. Strick, T., Allemand, J., Croquette, V. & Bensimon, D. (2000). Twisting and stretching single DNA molecules. *Prog. Biophys. Mol. Biol.* **74**, 115–140.

77. Strick, T. R., Allemand, J. F., Bensimon, D. & Croquette, V. (1998). Behavior of supercoiled DNA. *Biophys. J.* **74**, 2016–2028.

78. Strick, T. R., Croquette, V. & Bensimon, D. (1998). Homologous pairing in stretched supercoiled DNA. *Proc. Natl Acad. Sci. USA*, **95**, 10579–10583.

79. Strick, T. R., Croquette, V. & Bensimon, D. (2000). Single-molecule analysis of DNA uncoiling by a type II topoisomerase. *Nature*, **404**, 901–904.

80. Crisona, N. J., Strick, T. R., Bensimon, D., Croquette, V. & Cozzarelli, N. R. (2000). Preferential relaxation of positively supercoiled DNA by *E. coli* topoisomerase IV in single-molecule and ensemble measurements. *Genes Dev.* **14**, 2881–2892.

81. Dekker, N. H., Rybenkov, V. V., Duguet, M., Crisona, N. J., Cozzarelli, N. R., Bensimon, D. &

Croquette, V. (2002). The mechanism of type IA topoisomerases. *Proc. Natl Acad. Sci. USA*, **99**, 12126–12131.

82. Wenner, J. R., Williams, M. C., Rouzina, I. & Bloomfield, V. A. (2002). Salt dependence of the elasticity and overstretching transition of single DNA molecules. *Biophys. J.* **82**, 3160–3169.

83. Leger, J. F., Romano, G., Sarkar, A., Robert, J., Bourdieu, L., Chatenay, D. & Marko, J. F. (1999). Structural transitions on a twisted and stretched DNA molecule. *Phys. Rev. Letters*, **83**, 1066–1069.

84. Rief, M., Clausen-Schaumann, H. & Gaub, H. E. (1999). Sequence-dependent mechanics of single DNA molecules. *Nature Struct. Biol.* **6**, 346–349.

85. Clausen-Schaumann, H., Rief, M., Tolksdorf, C. & Gaub, H. E. (2000). Mechanical stability of single DNA molecules. *Biophys. J.* **78**, 1997–2007.

86. Lee, G. U., Chrisey, L. A. & Colton, R. J. (1994). Direct measurement of the forces between complementary strands of DNA. *Science*, **266**, 771–773.

87. Noy, A., Vezenov, D. V., Kayyem, J. F., Meade, T. J. & Lieber, C. M. (1997). Stretching and breaking duplex DNA by chemical force microscopy. *Chem. Biol.* **4**, 519–527.

88. Leuba, S. H., Karymov, M. A., Liu, Y., Lindsay, S. M. & Zlatanova, J. (1999). Mechanically stretching single chromatin fibers. *Gene Ther. Mol. Biol.* **4**, 297–301.

89. Leuba, S. H., Zlatanova, J., Karymov, M. A., Bash, R., Liu, Y.-Z., Lohr, D., Harrington, R. E. & Lindsay, S. M. (2000). The mechanical properties of single chromatin fibers under tension. *Single Mol.* **1**, 185–192.

90. Rief, M., Gautel, M., Oesterhelt, F., Fernandez, J. M. & Gaub, H. E. (1997). Reversible unfolding of individual titin immunoglobulin domains by AFM. *Science*, **276**, 1109–1112.

91. Oberhauser, A. F., Marszalek, P. E., Erickson, H. P. & Fernandez, J. M. (1998). The molecular elasticity of the extracellular matrix protein tenascin. *Nature*, **393**, 181–185.

92. Cui, Y. & Bustamante, C. (2000). Pulling a single chromatin fiber reveals the forces that maintain its higher-order structure. *Proc. Natl Acad. Sci. USA*, **97**, 127–132.

93. Brower-Toland, B. D., Smith, C. L., Yeh, R. C., Lis, J. T., Peterson, C. L. & Wang, M. D. (2002). Mechanical disruption of individual nucleosomes reveals a reversible multistage release of DNA. *Proc. Natl Acad. Sci. USA*, **99**, 1960–1965.

94. Luger, K. & Richmond, T. J. (1998). DNA binding within the nucleosome core. *Curr. Opin. Struct. Biol.* **8**, 33–40.

95. Widom, J. (1998). Structure, dynamics, and function of chromatin *in vitro*. *Annu. Rev. Biophys. Biomol. Struct.* **27**, 285–327.

96. Yin, H., Wang, M. D., Svoboda, K., Landick, R., Block, S. M. & Gelles, J. (1995). Transcription against an applied force. *Science*, **270**, 1653–1657.

97. Wang, M. D., Schnitzer, M. J., Yin, H., Landick, R., Gelles, J. & Block, S. M. (1998). Force and velocity measured for single molecules of RNA polymerase. *Science*, **282**, 902–907.

98. Wuite, G. J., Smith, S. B., Young, M., Keller, D. & Bustamante, C. (2000). Single-molecule studies of the effect of template tension on T7 DNA polymerase activity. *Nature*, **404**, 103–106.

99. Maier, B., Bensimon, D. & Croquette, V. (2000). Replication by a single DNA polymerase of a

stretched single-stranded DNA. *Proc. Natl Acad. Sci. USA*, **97**, 12002–12007.

100. Tahirov, T. H., Temiakov, D., Anikin, M., Patlan, V., McAllister, W. T., Vassylyev, D. G. & Yokoyama, S. (2002). Structure of a T7 RNA polymerase elongation complex at 2.9 Å resolution. *Nature*, **420**, 43–50.

101. Yin, Y. W. & Steitz, T. A. (2002). Structural basis for the transition from initiation to elongation transcription in T7 RNA polymerase. *Science*, **298**, 1387–1395.

102. Zhang, G., Campbell, E. A., Minakhin, L., Richter, C., Severinov, K. & Darst, S. A. (1999). Crystal structure of *Thermus aquaticus* core RNA polymerase at 3.3 Å resolution. *Cell*, **98**, 811–824.

103. Cramer, P., Bushnell, D. A. & Kornberg, R. D. (2001). Structural basis of transcription: RNA polymerase II at 2.8 angstrom resolution. *Science*, **292**, 1863–1876.

104. Gnatt, A. L., Cramer, P., Fu, J., Bushnell, D. A. & Kornberg, R. D. (2001). Structural basis of transcription: an RNA polymerase II elongation complex at 3.3 Å resolution. *Science*, **292**, 1876–1882.

105. Uptain, S. M., Kane, C. M. & Chamberlin, M. J. (1997). Basic mechanisms of transcript elongation and its regulation. *Annu. Rev. Biochem.* **66**, 117–172.

106. von Hippel, P. H. (1998). An integrated model of the transcription complex in elongation, termination, and editing. *Science*, **281**, 660–665.

107. Myers, L. C. & Kornberg, R. D. (2000). Mediator of transcriptional regulation. *Annu. Rev. Biochem.* **69**, 729–749.

108. Ebright, R. H. (2000). RNA polymerase: structural similarities between bacterial RNA polymerase and eukaryotic RNA polymerase II. *J. Mol. Biol.* **304**, 687–698.

109. Bennink, M. L., Pope, L. H., Leuba, S. H., de Grooth, B. G. & Greve, J. (2001). Single chromatin fibre assembly using optical tweezers. *Single Mol.* **2**, 91–97.

110. Leuba, S. H., Karymov, M. A., Tomschik, M., Ramjit, R., Smith, P. & Zlatanova, J. (2003). Assembly of single chromatin fibers depends on the tension in the DNA molecule: magnetic tweezers study. *Proc. Natl Acad. Sci. USA*, **100**, 495–500.

111. Widom, J. (1999). Equilibrium and dynamic nucleosome stability. In *Methods in Molecular Biology* (Becker, P. B., ed.), vol. 119, pp. 61–77, Humana Press, Totowa, NJ.

112. Allen, M. J., Dong, X. F., O'Neill, T. E., Yau, P., Kowalczykowski, S. C., Gatewood, J. *et al.* (1993). Atomic force microscope measurements of nucleosome cores assembled along defined DNA sequences. *Biochemistry*, **32**, 8390–8396.

113. Tomschik, M., Karymov, M. A., Zlatanova, J. & Leuba, S. H. (2001). The archaeal histone-fold protein HMf organizes DNA into *bona fide* chromatin fibers. *Struct. Fold. Des.* **9**, 1201–1211.

114. De Murcia, G. & Koller, T. (1981). The electron microscope appearance of soluble rat liver chromatin mounted on different supports. *Biol. Cell.* **40**, 165–174.

115. Vesenka, J., Hansma, H., Siegerist, C., Siligardi, G., Schabtach, E. & Bustamante, C. (1992). Scanning force microscopy of circular DNA and chromatin in air and propanol. *SPIE*, **1639**, 127–137.

116. Fritzsche, W., Schaper, A. & Jovin, T. M. (1994). Probing chromatin with the scanning force microscope. *Chromosoma*, **103**, 231–236.

117. Fritzsche, W., Schaper, A. & Jovin, T. M. (1995).

Scanning force microscopy of chromatin fibers in air and in liquid. *Scanning*, **17**, 148–155.

118. Fritzsche, W. & Henderson, E. (1996). Scanning force microscopy reveals ellipsoid shape of chicken erythrocyte nucleosomes. *Biophys. J.* **71**, 2222–2226.

119. Fritzsche, W. & Henderson, E. (1997). Chicken erythrocyte nucleosomes have a defined orientation along the linker DNA—a scanning force microscopy study. *Scanning*, **19**, 42–47.

120. Zlatanova, J., Leuba, S. H., Yang, G., Bustamante, C. & van Holde, K. (1994). Linker DNA accessibility in chromatin fibers of different conformations: a reevaluation. *Proc. Natl Acad. Sci. USA*, **91**, 5277–5280.

121. d'Erme, M., Yang, G., Sheagly, E., Palitti, F. & Bustamante, C. (2001). Effect of poly(ADP-ribosyl)-ation and Mg^{2+} ions on chromatin structure revealed by scanning force microscopy. *Biochemistry*, **40**, 10947–10955.

122. Dunker, A. K., Lawson, J. D., Brown, C. J., Williams, R. M., Romero, P., Oh, J. S. *et al.* (2001). Intrinsically disordered protein. *J. Mol. Graph. Model.* **19**, 26–59.

123. Furrer, P., Bednar, J., Dubochet, J., Hamiche, A. & Prunell, A. (1995). DNA at the entry/exit of the nucleosome observed by cryoelectron microscopy. *J. Struct. Biol.* **114**, 177–183.

124. Bednar, J., Studitsky, V. M., Grigoryev, S. A., Felsenfeld, G. & Woodcock, C. L. (1999). The nature of the nucleosomal barrier to transcription: direct observation of paused intermediates by electron cryomicroscopy. *Mol. Cell*, **4**, 377–386.

125. Leforestier, A., Fudaley, S. & Livolant, F. (1999). Spermidine-induced aggregation of nucleosome core particles: evidence for multiple liquid crystalline phases. *J. Mol. Biol.* **290**, 481–494.

126. Leforestier, A., Dubochet, J. & Livolant, F. (2001). Bilayers of nucleosome core particles. *Biophys. J.* **81**, 2414–2421.

127. Simpson, R. T., Thoma, F. & Brubaker, J. M. (1985). Chromatin reconstituted from tandemly repeated cloned DNA fragments and core histones: a model system for study of higher order structure. *Cell*, **42**, 799–808.